Efficient intracavity frequency doubling of a passively mode-locked diode-pumped neodymium lanthanum scandium borate laser

B. Braun, C. Hönninger, G. Zhang, and U. Keller

Ultrafast Laser Physics, Institute of Quantum Electronics, Swiss Federal Institute of Technology, ETH Hönngerberg-HPT, Zürich, Switzerland CH-8093

F. Heine, T. Kellner, and G. Huber

Institute of Laser-Physics, University of Hamburg, Jungiusstrasse 9a, Hamburg, Germany D-20355

Received March 27, 1996

We passively mode locked a diode-pumped neodymium lanthanum scandium borate laser with an antiresonant Fabry–Perot saturable absorber and achieved 2.8-ps pulses at an average output power of 400 mW and a pump power of 1.2 W. With Ti:sapphire laser pumping we obtained pulses as short as 1.6 ps. Intracavity doubling produced 190 mW of 531-nm light for a diode-pump power of 1.2 W, resulting in a conversion efficiency of 48% with respect to the fundamental and 16% with respect to the diode-pump power. Noise characterization of the laser demonstrates a trade-off between high conversion efficiency and low intensity noise. © 1996 Optical Society of America

Many applications, such as ranging, printing, and displays, can benefit from visible-wavelength lasers. Second-harmonic generation (SHG) is one method to generate light in the visible. Intracavity SHG is attractive for the low to intermediate power regimes, where typical intensities are insufficient to obtain high efficiency in extracavity nonlinear conversion. However, intracavity SHG suffers from the "green problem,"[1] i.e., chaotic intensity noise, making these lasers inappropriate for many applications. Many methods have been demonstrated to overcome the green problem, such as operating the laser at a single frequency,[1] using an external resonator for SHG,[2–6] maintaining a sufficiently low conversion efficiency,[1,7,8] balancing the birefringence of gain and nonlinear crystal,[9,10] operating the laser with many (>100) longitudinal modes,[11] and mode locking the laser to phase lock the longitudinal modes together. Intracavity SHG of both actively[10,12–15] and passively mode-locked (i.e., Kerr lens mode-locked)[16] lasers has been demonstrated.

In this Letter we demonstrate efficient intracavity SHG of a passively mode-locked neodymium lanthanum scandium borate[17,18] (Nd:LSB) laser producing 190 mW of 531-nm light with a diode-pump power of 1.2 W. An antiresonant Fabry–Perot saturable absorber[19,20] (A-FPSA) provides self-starting passive mode locking and generates pulses as short as 2.8 ps with diode pumping and 1.6 ps with Ti:sapphire pumping at a wavelength of 1.062 μm. At a diode-pump power of 1.2 W, we obtained 400 mW of average output power at 1.062 μm, corresponding to a 48% fundamental-to-green and a 16% pump-to-green conversion efficiency.

For comparison, a single-frequency ring laser produced 780 mW of green light at a pump power of 4 W (19% pump-to-green conversion efficiency).[21] In addition, external-resonator SHG has produced 200 mW of green light at a diode-pump power of 1 W (20% pump-to-green conversion efficiency).[4] Both techniques demonstrate slightly higher conversion efficiencies but also require special features such as extremely low intracavity losses and an electronic feedback system for the coupled cavities. Previously reported pump-to-green conversion efficiencies of intracavity-doubled actively mode-locked lasers are as high as 5.5% for Nd:YAG,[10] 3.3% for Nd:YLF,[15] and 5.2% for Ti:sapphire lasers.[14] The pump-to-green efficiency of an intracavity-doubled passively mode-locked Ti:sapphire laser was ≈1%.[16]

Figure 1 shows the schematic of the laser. We used an end-pumped astigmatically compensated cavity with a flat–Brewster-cut Nd:LSB laser crystal

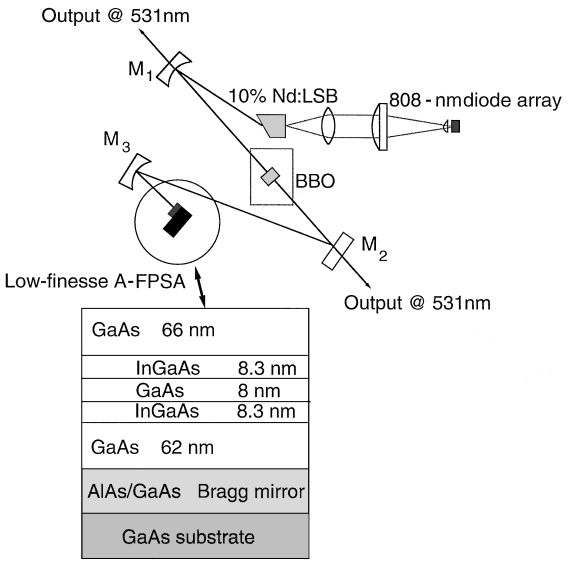

Fig. 1. Schematic of the experimental setup with the structure of the low-finesse A-FPSA (not to scale).

0146-9592/96/191567-03$10.00/0

that is 2.5 mm long and 10% doped. As a pump source we used a 2-W, 200-μm stripe-width diode array (SDL 2372 P1) at a lasing wavelength of 808 nm, which we focused to a 64 μm $\times$ 20 μm radius inside Nd:LSB. Close to 100% of the pump power was absorbed. We calculated the laser mode radius at the crystal flat to be 70 μm $\times$ 130 μm, using *ABCD* matrix formalism. The distance between curved mirror M_1 with a radius of curvature of 15 cm and the crystal was set to 10 cm. Thus a second focus of 180-μm radius was obtained between M_1 and M_2, at which we inserted the nonlinear crystal, a 7-mm-long antireflection-coated beta barium borate (BBO) crystal. We used BBO instead of KTP because type I phase matching in BBO maintains polarization, whereas type II phase matching in KTP can lead to depolarization of the fundamental. Another curved mirror, M_3, with a radius of curvature of 15 cm focuses the laser mode onto the A-FPSA to an $\approx$38-μm radius. For mode locking without intracavity SHG, M_1 is a high reflector and M_2 is a 2% output coupler for 1.06 μm (1% for each beam). For mode locking with intracavity SHG, mirrors M_1 and M_2 are coated for high reflection at the fundamental wavelength of 1.062 μm and for high transmission at the frequency-doubled wavelength of 531 nm. We therefore obtained two output beams for the intracavity-doubled light.

The saturable absorber in our laser (Fig. 1) is a low-finesse A-FPSA[22–24] that consists of a bottom reflector (25 pairs of AlAs/GaAs layers), two absorbing InGaAs quantum wells (8.3 nm thick) placed between transparent GaAs layers with a thickness adjusted for antiresonance, and a top reflector formed by the semiconductor–air interface. A nominal molecular beam epitaxy growth temperature of $\approx$350 °C reduces the recovery time of the A-FPSA to 8 ps, which was determined from a standard pump-probe technique by use of 200-fs pulses from a Nd:glass laser. Therefore the A-FPSA acts as a fast saturable absorber in the picosecond mode-locking regime. The position of the quantum wells is set to the peak of the intensity standing wave inside the A-FPSA to reduce the effective saturation fluence and maximize the modulation depth of the device for the available pump power. The modulation depth of the A-FPSA is $\approx$0.5%, sufficient for stable mode locking even with a SHG crystal inside the cavity. Because intracavity frequency doubling is a loss mechanism that is proportional to the laser peak intensity, it introduces higher loss for pulsed than for cw operation and is, therefore, a competing process to passive mode locking. Thus the intracavity SHG conversion efficiency per round trip has to be lower than the modulation depth of the A-FPSA. As we will discuss at the end, there is a trade-off between high conversion efficiency and low intensity noise for a given modulation depth of the saturable absorber. A higher conversion efficiency could be obtained with a higher modulation depth of the A-FPSA.

With no BBO crystal in the laser, we obtained stable, self-starting passively mode-locked pulses of 2.8 ps at 1.06 μm, a spectral width of 1.1 nm, or 290 GHz (Fig. 2), with an average output power of 400 mW at a pump power of 1.2 W. With Ti:sapphire laser pumping, we previously obtained pulses as short as 1.6 ps.[25] According to Fig. 2, the pulses are not transform limited and have a time–bandwidth product of 0.8, which is typical for enhanced spatial-hole burning in gain-at-the-end lasers[26,27] We measured a lasing pump threshold of 50 mW, a mode-locking threshold of 500 mW, and a cw slope efficiency of 32%. A small-signal gain coefficient of 0.76 for a pump power of 1.2 W can be determined[28] from the frequency of the relaxation oscillations at 166 kHz, an Nd:LSB upper-state lifetime of 120 μs,[18] a pulse-repetition rate of 177 MHz, and an estimated total cavity loss of $\approx$3%, taking into account the 2% output coupler and a nonsaturable 0.5% loss from the A-FPSA. The relaxation oscillations, and therefore the Q-switching instabilities, are typically suppressed by $\approx$90 dB below the carrier signal at the first harmonic of the mode-locked pulse train (Fig. 3).

With the BBO crystal in the laser, we measured a total average output power of 190 mW of TEM_{00} green light at 531 nm at a pump power of 1.2 W. The corresponding spectrum of the green light was measured in an optical microchannel analyzer and has a

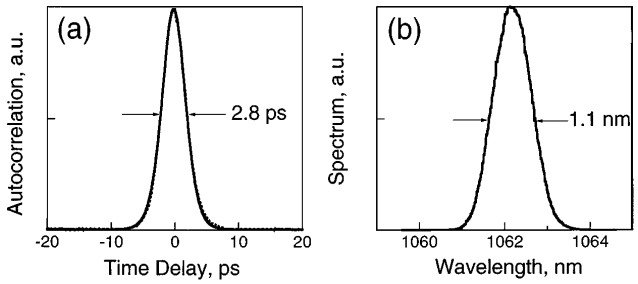

Fig. 2. Passive mode-locking results without intracavity frequency doubling: (a) noncollinear autocorrelation; (b) optical spectrum, resulting in a time–bandwidth product of 0.8.

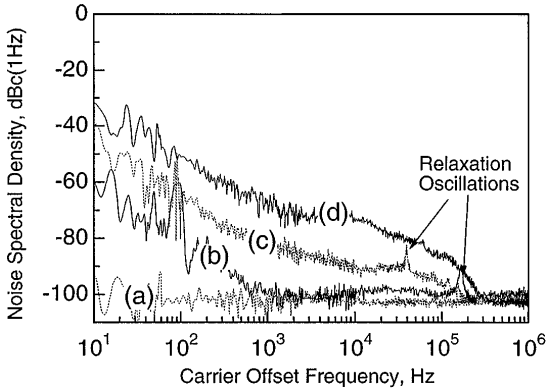

Fig. 3. Intensity noise spectral density measured with a photodiode and a microwave spectrum analyzer in dBc (1 Hz), i.e., the number of decibels below the first laser harmonic signal with a 1-Hz bandwidth. (a) The system noise floor (with the incident laser beam blocked at the photodiode). Also shown are noise sidebands for (b) the passively mode-locked Nd:LSB laser without the BBO crystal (0.8% rms noise integrated from 10 Hz to 1 MHz), (c) the intracavity-doubled green laser with 130-mW output power (2.5% rms noise integrated from 10 Hz to 1 MHz), and (d) the intracavity-doubled green laser with 190-mW output power (12% rms noise integrated from 10 Hz to 1 MHz).

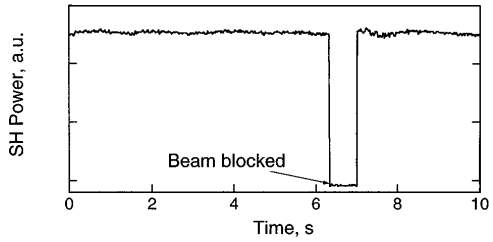

Fig. 4. Low-frequency green intensity noise at 190-mW power measured with a digital oscilloscope for 10 s with 500 data points.

FWHM of 0.37 nm, or 390 GHz, i.e., an $\sim\sqrt{2}$ broader spectrum for the SHG signal, which would indicate a $\sqrt{2}$ shorter pulse duration at 531 nm. However, we could not measure the pulse width because we did not have an autocorrelator for this wavelength. We obtain a fundamental-to-green conversion efficiency of 48%; this is the green power with respect to the fundamental power at 1.062 μm from the passively mode-locked Nd:LSB laser without the BBO crystal.

Figure 3 shows the single-sideband noise spectral density around the first laser harmonic at 177 MHz in units of dBc (1 Hz), i.e., the number of decibels below the carrier in a 1-Hz bandwidth, measured with a silicon photodiode and a microwave spectrum analyzer from 10 Hz to 1 MHz. Without the BBO crystal, the intensity noise [trace (b) in Fig. 3] rolls off below the system noise floor [trace (a) in Fig. 3] at a frequency offset of $\approx$1 kHz. The excess noise at higher frequencies is caused by the diode-pump laser. The rms intensity noise, integrated from 10 Hz to 1 MHz, is 0.8%. Intracavity doubling increases the intensity noise to $\approx$100 kHz. Figure 3 shows the noise sidebands for an average green output power of 130 mW [trace (c)] and 190 mW [trace (d)], where only the BBO crystal angle was slightly detuned to change the conversion efficiency. This measurement demonstrates the increase of intensity noise at higher conversion efficiencies. The rms intensity noise of the green beam, integrated from 10 Hz to 1 MHz, increased from 2.5% for 130 mW to 12% for 190 mW, where the conversion efficiency approached the modulation depth of the saturable absorber. The low-frequency peak-to-peak intensity noise of the 190-mW green light was 6.3%, as measured with a digital oscilloscope over 10 s with 500 data points, i.e., with integrated noise from 0.1 to 50 Hz (Fig. 4). A further increase of the conversion efficiency rapidly caused more intensity noise and at the end completely suppressed mode locking. At this point the green output power dropped drastically to a much lower value.

We have demonstrated both stable passive mode locking of a diode-pumped Nd:LSB laser and efficient intracavity frequency doubling. Pulses as short as 2.8 ps have been generated at 1.06 μm with no frequency-doubling crystal in the cavity. With a BBO crystal in the cavity, we obtained a green output power of 190 mW at 531 nm for a pump power of 1.2 W. The passive all-solid-state approach as well as the high conversion efficiency at a low pump power at relatively high pulse-repetition rates ($\approx$180 MHz) makes this visible light source potentially interesting for projection display applications.

This research was supported by the Swiss priority program in optics and the German Ministry of Education and Research.

References

1. T. Baer, J. Opt. Soc. Am. B **3,** 1175 (1986).
2. A. Askin, G. D. Boyd, and J. M. Dziedzic, IEEE J. Quantum Electron. **QE-2,** 109 (1966).
3. W. J. Kozlovsky, C. D. Nabors, and R. L. Byer, IEEE J. Quantum Electron. **24,** 913 (1988).
4. D. C. Gerstenberger, Lett. **16,** 992 (1991).
5. G. P. A. Malcolm, M. Ebrahimzadeh, and A. I. Ferguson, IEEE J. Quantum Electron. **28,** 1172 (1992).
6. K. Fiedler, S. Schiller, R. Paschotta, P. Kürz, and J. Mlynek, Opt. Lett. **18,** 1786 (1993).
7. N. MacKinnon and B. D. Sinclair, Opt. Commun. **105,** 183 (1994).
8. J.-P. Meyn and G. Huber, in *Conference on Lasers and Elecro-Optics*, Vol. 15 of 1995 OSA Technical Digest Series (Optical Society of America, Washington, D.C., 1995), p. 78.
9. G. E. James, E. M. Harrell, C. Bracikowski, K. Wiesenfeld, and R. Roy, Opt. Lett. **15,** 1141 (1990).
10. L. R. Marshall, A. D. Hays, A. Kaz, and R. L. Burnham, IEEE J. Quantum Electron. **28,** 1158 (1992).
11. V. Magni, G. Cerullo, S. DeSilvestri, O. Svelto, L. J. Qian, and M. Danailov, Opt. Lett. **18,** 2111 (1993).
12. C. B. Hitz and L. M. Osterink, Appl. Phys. Lett. **18,** 378 (1971).
13. T. E. Dimmick, Opt. Lett. **14,** 677 (1989).
14. R. J. Ellingson and C. L. Tang, Opt. Lett. **17,** 343 (1992).
15. J. R. Lincoln and A. I. Ferguson, Opt. Lett. **19,** 1213 (1994).
16. S. Backus, M. T. Asaki, C. Shi, H. C. Kapteyn, and M. M. Murnane, Opt. Lett. **19,** 399 (1994).
17. S. A. Kutovoi, V. V. Laptev, and S. Y. Matsnev, Sov. J. Quantum Electron. **21,** 131 (1991).
18. J.-P. Meyn, T. Jensen, and G. Huber, IEEE J. Quantum Electron. **30,** 913 (1994).
19. U. Keller, D. A. B. Miller, G. D. Boyd, T. H. Chiu, J. F. Ferguson, and M. T. Asom, Opt. Lett. **17,** 505 (1992).
20. U. Keller, Appl. Phys. B **58,** 347 (1994).
21. M. K. Reed, M. K. Steiner-Shepard, and D. K. Negus, in *Advanced Solid State Lasers*, Vol. 1 of Trends in Optics and Photonics Series (Optical Society of America, Washington, D.C., 1996), paper WE 2.
22. L. R. Brovelli, I. D. Jung, D. Kopf, M. Kamp, M. Moser, F. X. Kärtner, and U. Keller, Electron. Lett. **31,** 287 (1995).
23. I. D. Jung, L. R. Brovelli, M. Kamp, U. Keller, and M. Moser, Opt. Lett. **20,** 1559 (1995).
24. S. Tsuda, W. H. Knox, E. A. de Souza, W. Y. Jan, and J. E. Cunningham, Opt. Lett. **20,** 1406 (1995).
25. B. Braun, U. Keller, J.-P. Meyn, G. Huber, and T. H. Chiu, in *Conference on Lasers and Electro-Optics*, Vol. 15 of 1995 OSA Technical Digest Series (Optical Society of America, Washington, D.C., 1995), p. 155.
26. B. Braun, K. J. Weingarten, F. X. Kärtner, and U. Keller, Appl. Phys. B **61,** 429 (1995).
27. F. X. Kärtner, B. Braun, and U. Keller, Appl. Phys. B **61,** 569 (1995).
28. K. J. Weingarten, B. Braun, and U. Keller, Opt. Lett. **19,** 1140 (1994).